Biochemistry and Molecular Biology Faculty Publications

Department of Biochemistry and Molecular Biology

3-31-1995

The Crystal Structure of Recombinant Human Neutrophil-activating Peptide-2 (M6L) at 1.9-Å Resolution

Michael G. Malkowski
Department of Biochemistry, Wayne State University School of Medicine

Jean Yang Wu
Department of Biochemistry, Wayne State University School of Medicine

Jerome B. Lazar
Cell and Molecular Biology Laboratory, Stanford Research Institute International, Menlo Park, California

Paul H. Johnson
Cell and Molecular Biology Laboratory, Stanford Research Institute International, Menlo Park, California

Brian FP Edwards
Department of Biochemistry, Wayne State University School of Medicine, bedwards@med.wayne.edu

Recommended Citation

The Crystal Structure of Recombinant Human Neutrophil-activating Peptide-2 (M6L) at 1.9-Å Resolution*

Michael G. Malkowski‡, Jean Yang Wu‡, Jerome B. Lazar§, Paul H. Johnson§, and Brian F. P. Edwards‡¶

From the ‡Department of Biochemistry, Wayne State University, Detroit, Michigan 48201 and the §Cell and Molecular Biology Laboratory, Stanford Research Institute International, Menlo Park, California 94025

Neutrophil-activating peptide-2 (NAP-2) is a 70-residue carboxyl-terminal fragment of platelet basic protein, which is found in the α-granules of human platelets. NAP-2, which belongs to the CXC family of chemokines that includes interleukin-8 and platelet factor 4, binds to the interleukin-8 type II receptor and induces a rise in cytosolic calcium, chemotaxis of neutrophils, and exocytosis. Crystals of recombinant NAP-2 in which the single methionine at position 6 was replaced by leucine to facilitate expression belong to space group P1 (unit cell parameters a = 40.8, b = 43.8, and c = 44.7 Å and α = 98.4°, β = 120.3°, and γ = 92.8°), with 4 molecules of NAP-2 (M_r = 7600) in the asymmetric unit. The molecular replacement solution calculated with bovine platelet factor 4 as the starting model was refined using rigid body refinement, manual fitting in solvent-leveled electron density maps, simulated annealing, and restrained least squares to an R-factor of 0.188 for 2 σ data between 7.0- and 1.9-Å resolution. The final refined crystal structure includes 265 solvent molecules. The overall tertiary structure, which is similar to that of platelet factor 4 and interleukin-8, includes an extended amino-terminal loop, three strands of antiparallel β-sheet arranged in a Greek key fold, and one α-helix at the carboxyl terminus. The Glu-Leu-Arg sequence that is critical for receptor binding is fully defined by electron density and exhibits multiple conformations.

Neutrophil-activating peptide-2 (NAP-2)[1] is a cleavage product of the platelet α-granule component, platelet basic protein (PBP) and its derivative, connective tissue-activating peptide III (CTAP-III) (Castor *et al.*, 1983; Walz and Baggiolini, 1990). NAP-2 corresponds to the carboxyl-terminal fragment of PBP, which is cleaved by monocyte-derived proteases, and gives rise to a single peptide of 70 amino acids with a M_r of 7600 (Walz and Baggiolini, 1989). CTAP-III and β-thromboglobulin (β-TG), an additional truncation product of PBP (Begg *et al.*, 1978), can also be cleaved by neutrophil cathepsin G to generate NAP-2 (Cohen *et al.*, 1992).

Members of the chemotactic cytokine family, which are collectively known as chemokines, have four conserved cysteine residues and are divided into two subfamilies according to the position of the first pair of cysteines, which are separated by one amino acid (CXC) or are adjacent (CC) (Baggiolini *et al.*, 1994; Baggiolini and Clark-Lewis, 1992). The members of the two subfamilies differ in their selectivity, with the CXC subfamily targeting neutrophils and the CC subfamily targeting monocytes (Baggiolini *et al.*, 1994). PBP and its successive cleavage products, CTAP-III, β-TG, and NAP-2, belong to the CXC subfamily. Other members of this CXC subfamily include platelet factor 4 (PF4) (Deuel *et al.*, 1977; Hermodson *et al.*, 1977); interleukin-8 (IL-8) (Sherry and Cerami, 1991; Baggiolini and Clark-Lewis, 1992); the growth-related proteins GROα, GROβ, and GROγ (Haskill *et al.*, 1990; Tekamp-Olson *et al.*, 1990); ENA-78, a neutrophil-activating peptide identified in the conditioned medium of stimulated human type II epithelial cell line A549 (Walz *et al.*, 1991); macrophage inflammatory protein-2 (Wolpe *et al.*, 1988); and interferon-γ-inducible peptide-10 (γIP-10) (Luster *et al.*, 1985).

Unlike its three natural precursors, PBP, CTAP-III, and β-TG, NAP-2 has powerful neutrophil-stimulating effects involved in inflammation (Walz *et al.*, 1989). NAP-2 behaves as a typical chemotactic receptor agonist, inducing a rise in cytosolic calcium, chemotaxis, and exocytosis at concentrations between 0.3 and 10 nM. NAP-2, which is approximately half as potent as IL-8 as a neutrophil activator (Walz *et al.*, 1989), is released mainly into the vasculature where platelet activation and aggregation occur, whereas IL-8 is formed within tissues. IL-8, NAP-2, GROα, and ENA-78 bind to common receptors on neutrophils (Walz *et al.*, 1989, 1991; Moser *et al.*, 1990, 1991) and share a highly conserved Glu-Leu-Arg (ELR) sequence at their amino-terminal end that has been shown to be critical for receptor binding (Hébert *et al.*, 1991; Clark-Lewis *et al.*, 1991; Moser *et al.*, 1993). Comparable neutrophil responses were not observed with PF4 (Walz *et al.*, 1989; Lenord *et al.*, 1991), although chemotaxis and exocytosis have been reported with concentrations that were 1000–10,000-fold higher than those required for IL-8 (Deuel *et al.*, 1981; Bebawy *et al.*, 1986; Park *et al.*, 1990). No neutrophil-stimulating or other biological activities have been observed with γIP-10 (Dewald *et al.*, 1992).

Recent experiments have suggested that post-translationally modified forms of CTAP-III and NAP-2 can function as endoglucosamidases that degrade heparin and heparan sulfate to dimers (Hoogewerf *et al.*, 1993). Chondroitin and dermatan sulfates are not cleaved. This discovery further suggests a possible role for NAP-2 in the breakdown of basement membranes that occurs during metastasis, angiogenesis, and arthritis.

No other structure of NAP-2 is available, although the crys-

[1] The abbreviations used are: NAP-2, neutrophil-activating peptide; PBP, platelet basic protein; CTAP, connective tissue-activating peptide; β-TG, β-thromboglobulin; PF4, platelet factor 4; IL-8, interleukin-8; GRO, growth-related protein; γIP-10, interferon-γ-inducible peptide-10; HPLC, high pressure liquid chromatography.

tallization of recombinant NAP-2 was recently reported (Kungl *et al.*, 1994). However, crystal structures of bovine PF4 (St. Charles *et al.*, 1989), IL-8 (Baldwin *et al.*, 1991), and recombinant human PF4 (Stuckey, 1992; Zhang *et al.*, 1994) have been elucidated. The structure of IL-8 has been determined by NMR methods as well (Clore *et al.*, 1990). In all cases, the secondary structure of the monomer consists of an extended loop, three strands of antiparallel β-sheet folded in a Greek key, and one α-helix at the carboxyl terminus of the protein. In solution, IL-8 exists as a dimer in which the two monomers form an extended six-stranded β-sheet (Clore *et al.*, 1990). In the crystal structure of IL-8, the dimer lies on a crystallographic two fold so there is only a monomer in the asymmetric unit. PF4, which exists primarily as a tetramer in solution, formed orthorhombic crystals with a tetramer in the asymmetric unit that was formed by the back-to-back association of the extended β-sheets of two dimers (St. Charles *et al.*, 1989). In this paper, we present a refined crystal structure of biologically active, recombinant human NAP-2 {M6L}[2] in which methionine at position 6 in the NAP-2 sequence has been replaced by leucine to facilitate expression (Castor *et al.*, 1990). The crystal structure contains a PF4-like tetramer in the asymmetric unit of the triclinic unit cell.

MATERIALS AND METHODS

Preparation of Recombinant NAP-2—*Escherichia coli* cells were transformed with the pBR-CRM-CTAP-Met20,Leu26 {M15,L21} plasmid, which coded for a modified form of CTAP-III that had Met-20 replacing tyrosine and Leu-26 replacing methionine (Waleh *et al.*, 1992). Cleavage at Met-20 in CTAP-III with CNBr generates the amino terminus of native NAP-2, while the M26L substitution prevents the generation of a truncated form of NAP-2. Transformed *E. coli* cells were grown in shaker flasks in Luria broth containing 50 μg/ml ampicillin at 37 °C. CTAP (Met-20,Leu-26) protein expression was induced at an A_{660} of 0.4 by the addition of mitomycin C to a final concentration of 1 μg/ml. Cells were harvested and lysed by suspension in 6 M guanidine HCl, 0.1 M Tris-HCl (pH 8.0), 10 mM EDTA, and 6 mM sodium thiosulfate to protect against oxidation of cysteine by CNBr. The solution was purged with argon to remove oxygen, adjusted to 0.2 M in phosphoric acid and to 0.2 M in cyanogen bromide, and incubated overnight in the dark at room temperature. Besides generating free NAP-2 {M6L}, this treatment also aided in subsequent purification steps by fragmenting the endogenous *E. coli* proteins. The reaction mixture was dialyzed against deionized water to remove salts, CNBr, and sodium thiosulfate and freeze-dried.

The protein powder was dissolved and incubated for 1 h at 37 °C in 6 M guanidine HCl, 10 mM EDTA, 0.1 M dithiothreitol, 25 mM Tris-HCl (pH 8.6) to reduce disulfide bonds and to remove sulfonate-protecting groups from cysteine sulfhydryls. The solution was prepared for reverse-phase HPLC by acidification with 0.02 volumes of 88% formic acid, addition of 0.43 volumes of acetonitrile in 0.065% (v/v) trifluoroacetic acid, and centrifugation or filtration to remove any precipitate that formed. The reduced NAP-2 was purified on a Vydac 214TP1520 1-inch diameter reverse-phase column using a gradient that increased from 20% of eluant B to 35% at a rate of 0.1%/minute at a flow rate of 10 ml/min. Eluant A was water, and eluant B was acetonitrile (both 0.065% (v/v) in trifluoroacetic acid). The peak of reduced NAP-2 was pooled and lyophilized. NAP-2 was refolded at a concentration of 0.2 mg/ml in 2 M guanidine HCl, 0.1 M Tris-HCl (pH 8.6), 10 mM EDTA, 2 mM oxidized glutathione, 1 mM reduced glutathione at 37 °C for 2 h. The solution was acidified by the addition of 0.02 volumes of 88% formic acid and 0.33 volumes of acetonitrile. The filtered refolded NAP-2 was purified on a Vydac 214TP1022 high-resolution reversed-phase column

using the same gradient as described above. The NAP-2 peak was pooled and freeze-dried. Purity was judged to be >98% as assessed by spectral and amino acid composition analyses, amino-terminal sequencing, and analytical HPLC. Typical yields were 20–30 mg/liter of induced culture.

Crystallization—Crystals were grown by the hanging drop method at 22 °C from reservoirs containing 28% polyethylene glycol 4000, 100 mM sodium acetate (pH 4.6), and 200 mM ammonium acetate. The initial concentration of NAP-2 in the drop was 17 mg/ml. The crystals belong to space group P1 with unit cell dimensions of a = 40.8, b = 43.8, and c = 44.7 Å and $α$ = 98.4°, $β$ = 120.3°, and $γ$ = 92.8°, with four monomers in the asymmetric unit.

Data Collection—Diffraction data were collected at 22 °C on a single crystal (0.40 × 0.20 × 0.20 mm) mounted in a quartz capillary. The Siemens X-1000 area detector was mounted on a Rigaku RU200H rotating anode x-ray generator (CuK$_α$ radiation) that was operated at 40 kV and 70 mA and equipped with a Supper graphite monochromator. The data collection, which was organized using the program ASTRO (Chambers *et al.*, 1992), was done in eight sweeps of 280 frames/sweep at 0.25°/frame. Each frame was collected for 3 min to ensure that it contained at least one million total counts. The data were merged and scaled using the program XENGEN (Howard *et al.*, 1987), yielding 30,511 reflections, 17,830 of which were unique between 7.0 and 1.9 Å. These data, which represent 86.7% of the possible reflections, had an overall unweighted absolute R_{sym} of 0.025 based on intensities. For the three shells, 7.0 to 2.1, 2.1 to 2.0, and 2.0 to 1.9 Å, the completeness percentages were 97, 85, and 47%, respectively.

Molecular Replacement—The structure was solved by the molecular replacement method (Rossman and Blow, 1962) using the XPLOR suite of programs (Brunger, 1988) with a previously determined structure of PF4 as the model (St. Charles *et al.*, 1989). Because the sequence identity between the model and NAP-2 is 50%, residues that were not identical between structures were changed to alanine. The model tetramer was then placed in a 100-Å P1 orthogonal unit cell with its center of mass placed at the origin. The cross-rotation function was calculated for the range $θ_1$ = 0–360°, $θ_2$ = 0–180°, and $θ_3$ = 0–360° (Rao *et al.*, 1980) using the data between 7.0 and 4.0 Å. Patterson correlation refinement (Brunger, 1988) of the 150 most significant solutions identified two rotations, related by 179.5°, whose coefficients were above 0.43; the third best rotation had a correlation coefficient of 0.35. The first rotation ($θ_1$ = 297.2°, $θ_2$ = 13.9°, and $θ_3$ = 40.4°) was used to orient the model in the crystallographic unit cell. For convenience, the model was translated by x = 0.5, y = 0.5, and z = 0.5, so that roughly one tetramer would be contained within the limits of the unit cell. No translation function was calculated because there is only one tetramer in the P1 unit cell. The initial R-factor was 0.539 for data from 7.0- to 3.0-Å resolution.

Structural Analysis—The coordinates for the crystal structure of human IL-8 (entry 3IL8) and for the NMR structure of IL-8 (entry 1IL8) were obtained from the Protein Data Bank (Bernstein *et al.*, 1977). The coordinates for bovine PF4 were obtained from those of St. Charles *et al.* (1989) by refinement against diffraction data collected to 2.2-Å resolution from crystals of bovine PF4 that were free of nickel tetracyanate ions (Stuckey, 1992). The R-factor is 0.20. The coordinates for human PF4 were obtained by molecular replacement using the bovine coordinates and subsequent refinement to an R-factor of 0.19 at 2.0-Å resolution (Stuckey, 1992). Subunit B in NAP-2 was taken as the reference structure because its amino terminus has the fewest crystal contacts. Hydrogen bonds and surface accessibility values were calculated using the program QUANTA (Polygen Corp., Waltham, MA). The criteria for a hydrogen bond are that the angles C=O . . . H, O . . . H–N, and H–N–C be greater than 90 °C and the distance N . . . O not exceed 3.3 Å for a "short" hydrogen bond and 4.0 Å for a "long" one (Baker and Hubbard, 1984). Superposition of coordinates between structures was done using the program ALIGN (Satow *et al.*, 1986). Omit maps were calculated in XPLOR.

RESULTS

Structure Solution and Refinement—After 200 cycles of rigid body refinement, allowing the β-sheet and helical domains to refine independently, and fixing a different monomer in the tetramer every 50 cycles, the R-factor fell to 0.47 for data from 7.0 to 3.0 Å. Omit maps were calculated, in which a monomer was deleted from the tetramer, to see that the density for the deleted monomer was still present. Convinced that the solution gave a reasonable difference map, we proceeded directly to

---

[2] The residues of NAP-2 and the other chemokines are identified in the text by the three-letter code for amino acids and the equivalent position of the residue in the sequence of bovine platelet factor 4 (Fig. 1). Where appropriate, residues are also identified between braces by the one-letter code and the position of the residue in its own sequence. By this convention, the 70 residues in NAP-2 extend from Ala-21 {A1} to Asp-90 {D70}. We use residue positions 21–90 when speaking generally of all four subunits. Specific residues in the separate subunits of the NAP-2 tetramer are distinguished by subscripts, for example, sequence numbers 21^a–90_a for subunit A.

```
                    1     5        10        15          20          25          30            35
      B-PF4   E S S F P A T F V P L P A D S E G G E D E D L Q C V C L K T T S G - │I│N
      H-PF4                 E A E E D G D L Q C L C V K T T S Q - │V│R
      NAP-2                           A│E L R│C M C I  K T T S G - │I│H
      H-IL8                       S A K│E L R│C Q C I  K T Y S K P│F│H
     ENA-78           A G P A A A V L R│E L R│C V C L Q T T Q G - │V│H
     GROα                         A S V A T│E L R│C Q C L Q T L Q G - │I│H
     MIP-2                         A V V A S│E L R│C Q C L K T L P - R│V│D
     γIP-10                        V P L S R T V R C T C I  S I  - N Q P│V│N
                                    1           5        10          15
```

```
                        40          45        50          55          60            65          70
      B-PF4   P R H│I│S S│L│E│V│I│G A G T H C P S P Q│L│L│A T K K T - G R K│I│ │C│L│D Q
      H-PF4   P R H│I│T S│L│E│V│I│K A G P H C P T A Q│L│I│A T L K N - G R K│I│ │C│L│D L
      NAP-2   P K N│I│Q S│L│E│V│I│G K G T H C N Q V E│V│I│A T L K D - G R K│I│ │C│L│D P
      H-IL8   P K F│I│K E│L│R│V│I│E S G P H C A N T E│I│I│V K L S D - G R E│L│C│L│D P
     ENA-78   P K M│I│S N│L│Q│V│F│A I  G P Q C S K V E│V│V│A S L K N - G K E│I│ │C│L│D P
     GROα     P K N│I│Q S│V│N│V│K S P G P H C A Q T E│V│I│A T L K N - G R K A C│L│N P
     MIP-2    F K N│I│Q S│L│S│V│T P P G P H C A N T E│I│I│V K L S D - G R E│L│C│L│D P
     γIP-10   P R S│L│E K│L│E│I│I│P A S Q F C P R V E│I│I│A T M K K K G E K R C│L│N P
                    20          25          30          35        40          45          50
```

```
                        75          80          85        90
      B-PF4   Q R P L Y K K│I│L│K K L│L│D G D E S
      H-PF4   Q A P L Y K K│I│I│K K L│L│E S
      NAP-2   D A P R I  K K│I│V│Q K K│L│A G D E S A D
      H-IL8   K E N W V Q R│V│V│E K F│L│K R A E N S
     ENA-78   E A P F L K K│V│I│Q K I │L│D G G N K E N
     GROα     A S P I  V K K│I│I│E K M│L│N S D K S N
     MIP-2    K E N W V Q R│V│V│E K F│L│K R A E N S
     γIP-10   E S K A I  K N│L│L│K A V S K E M S K R S P
                    55          60          65          70
```

FIG. 1. **Sequence homology within the chemokine CXC subfamily.** The sequences have been aligned to show the conservation of the four cysteine residues. The sequence of NAP-2 is compared to other known proteins belonging to the CXC family, namely human IL-8 (Sherry and Cerami, 1991; Baggiolini and Clark-Lewis, 1992), ENA-78 (Walz et al., 1991), GROα (Haskill et al., 1990; Tekamp-Olson et al., 1990), macrophage inflammatory protein-2 (Wolpe et al., 1988), bovine (Ciaglowski et al., 1986) and human (Poncz et al., 1987) PF4, and γIP-10 (Luster et al., 1985). The conserved ELR sequence and the 12 structurally conserved hydrophobic residues are *boxed*. The residue positions in PF4 are in *boldface* above the sequences, and the corresponding numbers in IL-8 are given below.

simulated annealing utilizing the slow cool annealing protocol in XPLOR. The dynamics temperature started out at 4000 K and decreased in intervals of 25 K to a final temperature of 0 K with 25 steps (0.5 fs/step) of Verlet dynamics at each temperature. This reduced the R-factor to 0.328 using all the data from 7.0 to 1.9 Å. Side chains in subunit A that had been replaced by alanine in the model were then placed into an electron density map that was calculated with a locally written program to perform noncrystallographic symmetry averaging.[3] Positional refinement and analysis of electron density maps that were improved through solvent leveling, histogram matching, and Sayre's equations using the program SQUASH (Zhang, 1993) were then used to fit additional residues at the amino and carboxyl termini of the individual subunits and to adjust poorly fit side chains. The R-factor was reduced to 0.234 for all the data from 7.0 to 1.9 Å.

At this point, all the residues were fit to well defined density with the exception of the last four carboxyl-terminal residues in each subunit and the three amino-terminal residues in subunit C, which were disordered. These residues were removed before proceeding with further refinement. Water molecules were then added at positions that were within 2.5–3.5 Å of a hydrogen bonding donor or acceptor and had electron density in both $F_o - F_c$ and $2F_o - F_c$ maps. A total of 145 cycles of GPRLSA refinement (Furey et al., 1982), including 265 water molecules, dropped the R-factor to 0.202 for 2 σ data from 7.0 to 1.9 Å, with root mean square deviations for bonds and ω angles of 0.020 Å and 5.5°, respectively (Table I). Finally, the XPLOR program

TABLE I
Refinement statistics from GPRLSA

Total no. of atoms	2251
No. of solvent atoms	265
No. of observations	17475
Mean isotropic B (Å^2)	30.5
Root mean square deviations	
Bond distances (Å)	0.020
Angle distances (Å)	0.038
1–4 distances (Å)	0.041
Bond angles (degrees)	1.3
915 peptide planes (Å)	0.0100
Chiral volume (Å^3)	0.127
Single torsion contacts (Å)	0.206
Multiple torsion contacts (Å)	0.339
Possible ($X \ldots Y$) H bond contacts (Å)	0.364
Planar (ω) torsion angles (degrees)	5.5
Staggered torsion angles (degrees)	20.3
Orthonormal torsion angles (degrees)	43.5
Final R-factor from GPRLSA	0.202
R-Factor from XPLOR (B refinement only)	0.188

was used to refine only the B values in each subunit. Twenty-five cycles of B refinement dropped the R-factor to 0.188 for data from 7.0 to 1.9 Å and greater than 2 σ.

The final refined model of the 4 molecules of NAP-2 in the asymmetric unit (Fig. 2) has excellent stereochemistry when evaluated with the program PROCHECK (Morris et al., 1992). On the Ramachandran plot, 90.5% of the residues are in the most favored region, and none lie in the disallowed region. Other well refined structures at an equivalent resolution have 83.8% of their residues, on average, within the most favored region. The nine other parameters evaluated by PROCHECK
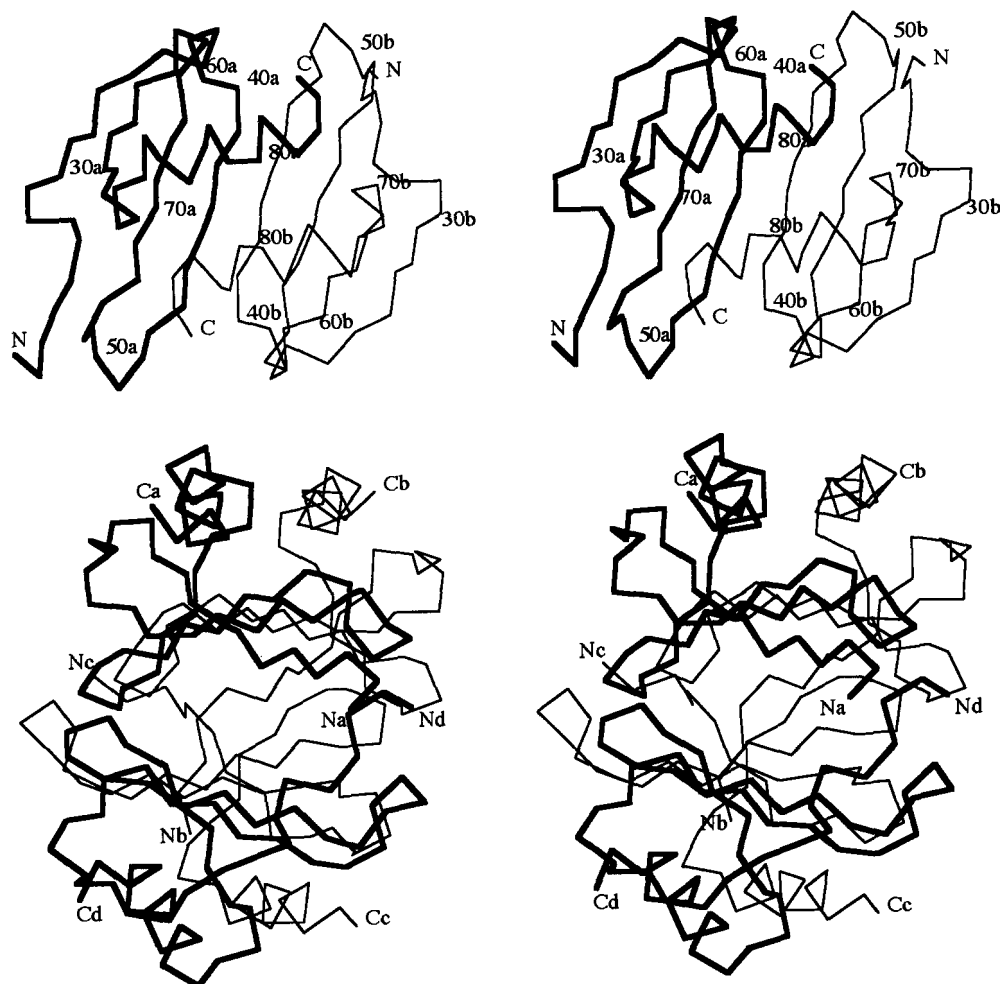
---

[3] P. Martin, unpublished data.

FIG. 2. **Structure of NAP-2.** *Top*, the α-carbon backbones of residues 21_a-86_a (*thick lines*) and of residues 21_b-86_b (*thin lines*) are shown in stereo. The view is approximately down the AB noncrystallographic axis. *Bottom*, the α-carbon backbone of the NAP-2 tetramer is shown in stereo as viewed approximately down the AD noncrystallographic axis. As drawn, subunits A (*thick lines*) and B (*thin lines*) are above subunits C (*thin lines*) and D (*thick lines*).

are also equal to or better than the bounds established from well refined structures at equivalent resolution.

Secondary Structure of NAP-2—The secondary structure of NAP-2 is summarized in Fig. 3. The amino terminus, which starts at position 21 in each subunit, is ordered in subunits A, B, and D (Fig. 4), but Ala-21_c, Glu-22_c, and Leu-23_c are disordered in subunit C. Ala-21 to Ile-34 form a large open loop that is stabilized by the two disulfide bonds Cys-25–Cys-51 and Cys-27–Cys-67. Also, there are bends, as defined by Kabsch and Sander (1983), centered at residues 25 and 27 and one hydrogen bond from Thr-31 to Cys-67. A main chain hydrogen bond exists between the nitrogen of Asp-69 and the carbonyl oxygen of Thr-31, which also contributes to stabilize the loop. His-35 to Asn-38 form a single turn of 3_{10} helix in an external loop that is stabilized by main chain hydrogen bonds between Asn-38 and His-35 and between Ile-39 and Pro-36.

The first strand of the three-stranded β-sheet is formed by Ile-39 to Gly-46. There are six main chain hydrogen bonds formed with the adjacent subunit that form the extended six-stranded β-sheet (Fig. 3). Glu-43_a on the "interior side" of the β-sheet forms an internal salt bridge with Lys-65_c in the other extended β-sheet and similarly for the related pair Glu-43_c to Lys-65_a. The respective Glu-OE2 to Lys-NZ distances are 2.61 and 3.31 Å, respectively. The comparable salt bridges between subunits B and D, namely Glu-43_b–Lys-65_d and Glu-43_d–Lys-65_b, which have Glu-OE2 to Lys-NZ distances of 6.70 and 7.29

Å, respectively, are not made due to the absence of perfect 222 symmetry in the crystal packing.

Lys-47 to Gln-53 form a hairpin loop (Sibanda and Thornton, 1985) between strands I and II of the β-sheet. There is a 14-atom turn involving main chain hydrogen bonds formed between the nitrogen of Gly-48 and the oxygen of Cys-51 and between the nitrogen of Cys-51 and the oxygen of Gly-48. Strands II and III of the β-sheet are formed by Val-54 to Thr-59 and by Arg-64 to Leu-68, respectively. They are linked by Leu-60 to Gly-63, which form a hydrogen-bonded type I reverse turn. There are two β-bulges (Richardson, 1981): a wide type at Ile-39–Gln-40 and a G type at Gly-63–Arg-64.

Asp-69 to Arg-74 loop between strand III and the helix at the end of the molecule. There is a hydrogen bond between Asp-69 and Ala-72 that forms an inverse γ-turn (Rose *et al.*, 1985). Ile-75 to Asp-86 form an α-helix that lies diagonally across the top of the β-sheet.

Comparison of the 4 NAP2 Molecules—Although the 4 molecules of NAP-2 present in the asymmetric unit of our NAP-2 crystals are crystallographically independent and occupy nonequivalent environments, they all have the 15-residue open loop, three strands of antiparallel β-sheet, and the 12-residue helix lying across the pleated sheet as described above. The 4 molecules are paired to form two extended β-pleated sheets of six strands each (Fig. 2), which are then arranged back to back to form a tetramer with approximate dimensions of 35 × 35 ×

45 Å^3. The subunits of the tetramer are related by quasi *222* symmetry. The two six-stranded β-sheets that lie back to back in the tetramer are bisected by a perpendicular rotation axis that relates subunits A to B and subunits C to D with a rotation angle of 178.5° (ALIGN). The two rotation axes parallel to the

FIG. 3. **Hydrogen bonds and topology of NAP-2.** Main chain hydrogen bonds for the four loops, three strands of β-sheet, and one α-helix found in the NAP-2 monomer are shown as *arrows* going from the donor to the acceptor. The two disulfide bonds are indicated by *thick arrows*. Ala-72 to Lys-81 in the helical region are also acceptors in 3$_{10}$-type hydrogen bonds with the residue three positions farther along in the sequence. These hydrogen bonds are generally longer than the α-helical type and are not shown. A hydrogen bond was included in the diagram if it was present in all four subunits.

β-sheets relate subunits A to C and subunits B to D with a rotation angle of 179.4° and subunits A to D and subunits B to C with a rotation angle of 170.1°.

The individual molecules are similar to one another as evidenced by the average root mean square deviation of 0.47 Å in C-α positions when they are overlapped in pairs (Table II). In these six pairwise comparisons, the C-α atoms of 14 residues (Ala-21 to Arg-24, Ile-28, Lys-29, His-35, Gly-48 to His-50, Asn-52, and Ala-84 to Asp-86) were separated by more than twice the average root mean square deviation in at least one of the overlaps. The largest C-α deviations between the subunits (2.0–8.58 Å) occur at the amino terminus where Ala-21$_a$ to Arg-24$_a$ interact with residues in adjacent asymmetric units and consequently exhibit a markedly different conformation from the same residues in subunits B and D (Fig. 5). Only five of the 14 residues, namely Arg-24, Gly-48, Thr-49, Ala-84, and Asp-86, have C-α deviations greater than 0.94 Å that are not also associated with differences in packing contacts with other subunits, either in the same or adjacent asymmetric units. Among these five residues, Thr-49, which is part of the loop between β-strands I and II, has the largest C-α displacement (2.18 Å between subunits B and C) and exceeds 0.94 Å in all pairwise comparisons, except in the overlap of subunits A and C.

DISCUSSION

The secondary structure and main chain hydrogen bonding of NAP-2 as shown in Fig. 3 are very similar to those of the other known structures in the CXC chemokine family (St. Charles *et al.*, 1989; Baldwin *et al.*, 1991). Fig. 3 includes all of the hydrogen bonds identified in an NMR analysis of the β-sheet region of NAP-2 (Yang *et al.*, 1994) with the exception of the bond between the nitrogen of Arg-64 and the oxygen of Leu-60, which is a bond between the nitrogen of Gly-63 and the oxygen of Leu-60 in the x-ray structure, as well as three β-sheet hydrogen bonds that are not detected by NMR, namely the two bonds between Ile-45 and Glu-55 and the bond between the nitrogen of Ile-57 and the oxygen of Glu-43.

Tertiary and Quaternary Interactions—In addition to the disulfide and hydrogen bonds shown in Fig. 3, several clusters of hydrophobic residues contribute to the integrity of the subunits. For example, Ile-34$_a$ and Pro-36$_a$, which reside in the loop structure, cluster with Ile-39$_a$, Leu-42$_a$, Ile-66$_a$, and Leu-68$_a$ in the β-sheet and with Ile-75$_a$ and Ile-78$_a$ in the α-helix. At the helix-sheet interface, Leu-42$_a$ and Val-56$_a$ in the β-sheet contact Val-79$_a$ and the C-γ, C-δ, and C-ε atoms of Lys-82$_a$. Similarly, the dimer interface is strengthened by hydrophobic contacts between residues in each helix, for instance Val-79$_a$, Lys-82$_a$ (C-γ, C-δ, and C-ε), and Leu-83$_a$, and between residues in the β-sheet of the partner, Leu-42$_b$, Val-44$_b$, and Val-56$_b$. The overlap of the inner hydrophobic surfaces of the α-helices with the β-sheet strands from the adjacent monomer creates a shallow hydrophobic groove between the helices that has a floor
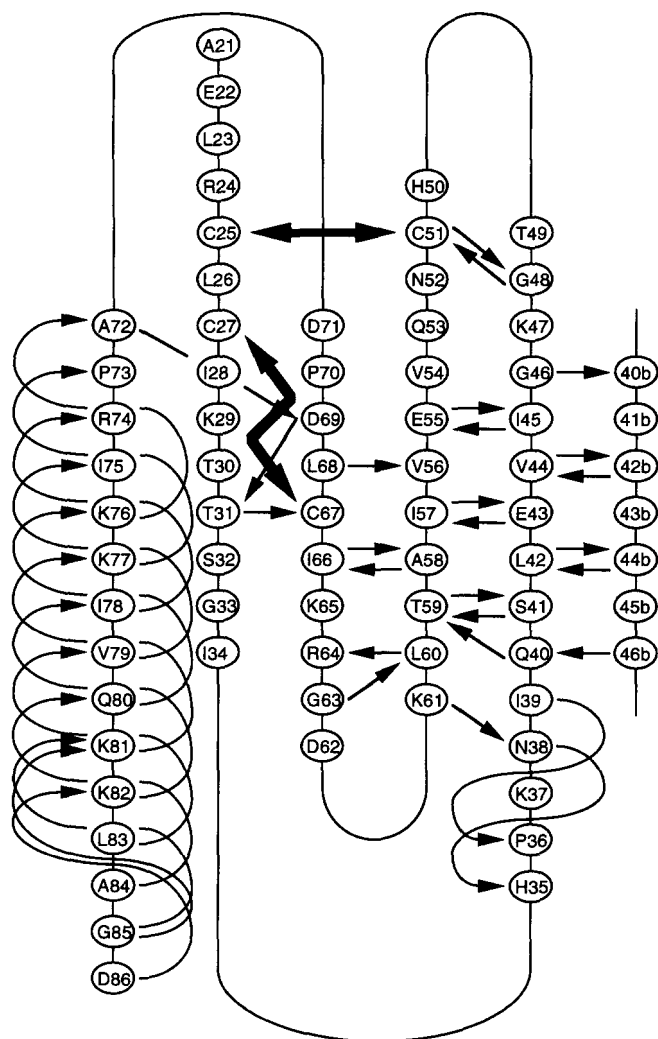

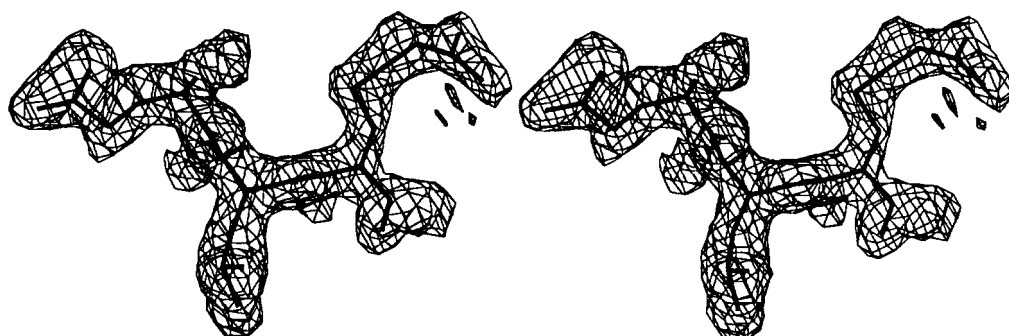FIG. 4. **Electron density for the ELR sequence of NAP-2.** The electron density in a $2F_o - F_c$ map contoured at 2 σ is shown in stereo for Glu-22$_a$, Leu-23$_a$, and Arg-24$_a$ in NAP-2. The final refined model is shown in *thick lines*.

defined by Leu-42$_a$, Val-44$_a$, Val-54$_a$, and Val-56$_a$ along with the equivalent residues in subunit B and walls defined by Pro-70$_a$, Ile-75$_a$, Lys-76$_a$ (side chain C-γ, C-δ, and C-ϵ atoms), Val-79$_a$, and Leu-83 along with the same residues from subunit B. The CD dimer has a similar groove.

The last four residues, Glu-87, Ser-88, Ala-89, and Asp-90, are disordered in the electron density maps of NAP-2 {M6L}. They are not part of the binding site for receptors (Clark-Lewis *et al.*, 1994), but when one to three of these residues are removed, the activity of NAP-2 increases 4-fold (Brandt *et al.*, 1993). Possibly, these residues inhibit the activity of NAP-2, which is most active as a monomer (Schnitzel *et al.*, 1994), by extending the α-helices farther across the adjacent β-sheets and thereby stabilizing the dimer interface.

TABLE II
Root mean square deviation of NAP-2 C-α coordinates from those of other chemokines

NAP-2 subunit(s)	Chemokine subunit(s)	β-Sheet[a]	α-Helix[b]	Overall
		$\mathring{A}$	$\mathring{A}$	$\mathring{A}$
NAP-2A	NAP-2C	0.346	0.217	0.343
NAP-2A	NAP-2D	0.434	0.206	0.499
NAP-2C	NAP-2D	0.608	0.267	0.652
NAP-2B[c]	NAP-2A	0.376	0.216	0.438
NAP-2B	NAP-2C	0.535	0.207	0.571
NAP-2B	NAP-2D	0.307	0.254	0.304
NAP-2B	PF4A (bovine)[d]	0.740	1.577	1.060
NAP-2B	PF4A (human)[d]	0.998	1.666	1.175
NAP-2B	IL-8 (x-ray)	1.113	0.328	0.939
NAP-2B	IL-8A (NMR)[d]	1.077	0.639	1.305
NAP-2AB	NAP-2CD	0.392	0.257	0.361
NAP-2AB	PF4AB (bovine)[d]	1.033	1.689	1.327
NAP-2AB	PF4AB (human)[d]	0.962	1.862	1.288
NAP-2AB	IL-8AB (x-ray)[e]	1.919	1.760	2.112
NAP-2AB[c]	IL-8AB (NMR)	1.431	3.248	2.254

[a] Residues 25–67.

[b] Residues 68–85.

[c] Subunit B was chosen as the reference structure because its amino terminus was not involved in crystal contacts.

[d] Overlaps with the other subunits of the chemokine gave similar values for the root mean square deviation.

[e] The IL-8 dimer (x-ray) was generated from crystallographic symmetry.

The interface of the AB and CD dimers also is stabilized through hydrophobic interactions. Leu-26$_a$ clusters with its counterpart, Leu-26$_c$, and also with Ile-57$_c$ and the side chain C-γ, C-δ, and C-ϵ atoms of Lys-65$_c$. Ile-45$_a$ in the β-sheet also interacts with the C-γ, C-δ, and C-ϵ atoms of Lys-65$_c$. Similarly, Leu-26$_b$ contacts Leu-26$_d$. However, the interface between the two dimers, which contains the four buried salt links discussed earlier, appears to be predominantly hydrophilic in that 18 of the 22 residues in the CD dimer that are within 3.5 Å of a residue in the AB dimer are hydrophilic.

Additional evidence for structural significance of the residues mentioned above comes from the similarity between the specific residues in NAP-2 and residues in homologous proteins within the chemokine family (Fig. 1). The potential for salt links between Glu-43$_a$ and Lys-65$_c$ and between Lys-65$_a$ and Glu-43$_c$ is conserved in bovine PF4, human PF4, and γIP-10, while in IL-8, the acidic and basic residues have switched positions, with lysine replaced by arginine at position 43. Also, almost all of the hydrophobic residues mentioned above as having important structural roles in NAP-2 occupy the same positions throughout the chemokine family and are highly conserved.

One exception occurs at position 26, where wild-type NAP-2 has methionine and other chemokines have valine, leucine, threonine, or glutamine (Fig. 1). The hydrophobic contacts described above for Leu-26 in our NAP-2 structure, which replaces the wild-type methionine, suggest that a medium-sized hydrophobic residue at this position shifts the dimer/tetramer equilibrium toward tetramers. Human and bovine PF4, which have Leu-26 and Val-26, respectively, form tetramers in the crystal similar to those of our NAP-2 mutant and form mostly tetramers in solution (Bock *et al.*, 1980; Mayo and Chen, 1989), whereas NAP-2 and IL-8, which have Met-26 and Gln-26, respectively, exhibit a monomer/dimer/tetramer equilibrium in solution (Schnitzel *et al.*, 1994; Yang *et al.*, 1994). At physiological concentrations of 10^{-7} M and lower, both IL-8 and NAP-2 exist and act primarily as monomers (Rajarathnam *et al.*, 1994; Schnitzel *et al.*, 1994; Yang *et al.*, 1994), although protein cross-linking experiments indicate that IL-8 can also bind as an oligomer to its receptor (Schnitzel *et al.*, 1994). When
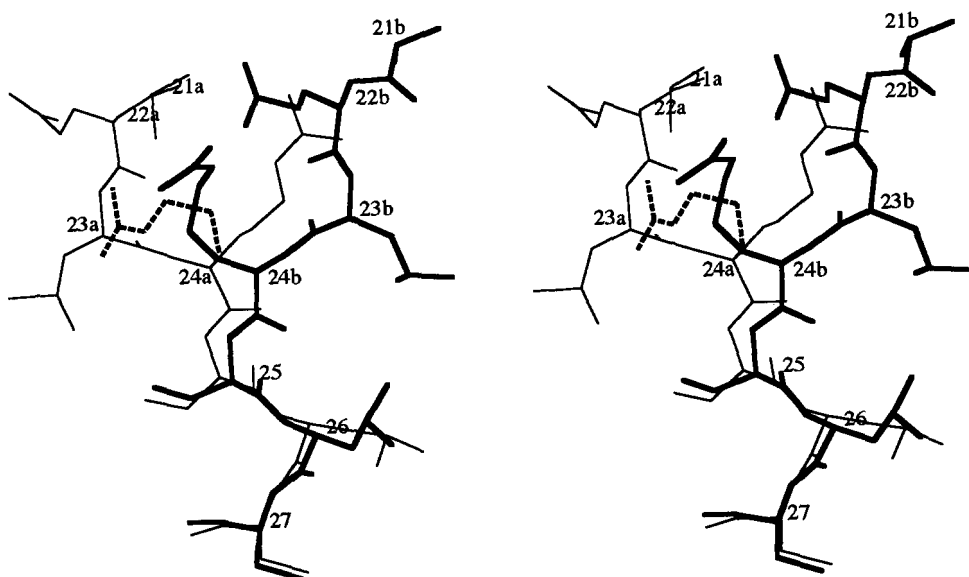

FIG. 5. **Conformation of the ELR sequence in the subunits of NAP-2.** The conformations of Ala-21, Glu-22, Leu-23, Arg-24, Cys-25, Leu-26, and Cys-27 are compared for subunits A (*thin lines*) and B (*thick lines*). The conformation of Arg-24$_b$ shown in *solid lines* is the one most similar to that present in subunit D; the conformation shown in *dashed lines* is an alternative conformation present in subunit B only. In subunit C, the first three residues are disordered, and the conformation of Arg-24$_c$ is similar to that of Arg-24$_b$ shown in *solid lines*. In subunit D, the four residues have a conformation similar to that shown for subunit B.
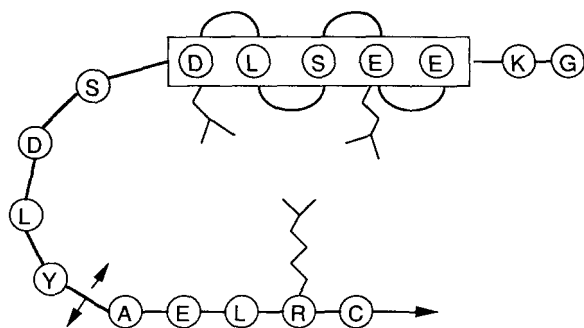
FIG. 6. **A model for the activation peptide of NAP-2.** A helix is predicted by the method of Holley and Karplus (1989) for Glu-12 to Asp-16 in the activation peptide of β-TG (Gly-10 to Tyr-20). The activation peptide, which presents two negatively charged side chains on one side of the helix, is shown bending back to interact with the ELR region of NAP-2. The activation peptide is released from β-TG to form NAP-2 by cleavage between Tyr-20 and Ala-21 (*dashed arrow*).

Gln-26 in IL-8 is replaced by leucine, it remains active (Clark-Lewis *et al.*, 1994), as does NAP-2 when Met-26 is replaced by leucine (Castor *et al.*, 1990).

ELR Region—The amino-terminal residues Glu-22, Leu-23, and especially Arg-24 have been identified in IL-8 as being important for receptor binding (Hébert *et al.*, 1991; Clark-Lewis *et al.*, 1991, 1993; Moser *et al.*, 1993). This ELR sequence, which is conserved in the chemokines NAP-2, GROα, and murine inflammatory protein-2 (Fig. 1), which compete with IL-8, is necessary but not sufficient for binding to the two classes of IL-8 receptors on neutrophils (Oppenheim *et al.*, 1991). For example, IL-8 binds tightly to both receptors, whereas the other chemokines bind tightly to only the type II receptor (Moser *et al.*, 1991; Holmes *et al.*, 1991; Murphy and Tiffany, 1991). When the ELR sequence is introduced into PF4 and γIP-10, the former acquires activity, but the latter does not (Clark-Lewis *et al.*, 1993). Besides the ELR motif, a compact tertiary structure with intact disulfide bonds is needed (Peveri *et al.*, 1988; Van Damme *et al.*, 1989) in addition to appropriate residues at positions 22–43, 47–52, and 66 (IL-8 residues 4–22, 30–35, and 49) (Clark-Lewis *et al.*, 1994).

The conformation of the amino-terminal ELR region is well defined in every subunit of NAP-2 except subunit C (Fig. 4), which lacks density for Ala-21$_3$ to Leu-23$_c$. However, the particular structure adopted by an ELR region depends strongly upon the local environment. The ELR regions of subunits A and B have very different structures (Fig. 5) because they are stabilized by different interactions: the former with a symmetry-related NAP-2 tetramer and the latter with subunit D in its own tetramer. Conversely, the ELR region of subunit D reciprocally interacts with subunit B in the same tetramer and adopts a conformation similar to that seen in subunit B. Because of crystal packing and asymmetry in the NAP-2 tetramer, neither interaction is accessible to the ELR region in subunit C, which is consequently disordered. Clearly, the main chains of the ELR regions exhibit unusual flexibility despite being tethered to the core of the protein through disulfide bridges at Cys-25 and Cys-27. Moreover, the side chain of Arg-24$_b$, which has no intra- or intermolecular contacts, exhibits two conformations, indicating that this critical residue in receptor binding also has intrinsic conformational flexibility (Fig. 5). At physiological concentrations, where NAP-2 probably functions as a monomer (Rajarathnam *et al.*, 1994; Schnitzel *et al.*, 1994; Yang *et al.*, 1994), the ELR region would be unconstrained by intermolecular interactions, much like the case with subunit C, and could adopt an extended conformation on the receptor if necessary.

The positions of the ELR residues in the IL-8 crystal struc-

ture (Baldwin *et al.*, 1991) match those in subunit B of NAP-2 better than in subunit A or D. The C-α atoms of the two leucine residues and the two arginine residues are separated by 3.65 and 1.11 Å, respectively (Glu-22 is not defined in the IL-8 crystal structure). Although Leu-23$_b$ and Arg-24$_b$ in NAP-2 and Leu-23 in the IL-8 crystal structure have no intermolecular contacts, the side chain of Arg-24 in IL-8 forms three hydrogen bonds with a symmetry-related molecule in the crystal. The first five amino-terminal residues in the IL-8 NMR structure are considered as being partially disordered due to a standard deviation of 5 Å in the atomic positions of these residues (Clore *et al.*, 1990). In the bovine PF4 crystal structure, the amino-terminal residues are disordered, and position 24, which is the first residue defined by electron density in the structure, is a Gln instead of Arg (St. Charles *et al.*, 1989).

It has also been suggested that Glu-22 {E4} in IL-8 may form a salt bridge with either Lys-40 {K23} or Lys-59 {K42} in the adjacent monomer of IL-8, but since neither lysine is critical for receptor binding, it is more likely that Glu-22 interacts with the receptor and not with the other subunit in the dimer (Hébert *et al.*, 1991). The equivalent residues in NAP-2 are Gln-40 and Thr-59, so no ion pair is possible in our structure. Ile-28 in IL-8 has also been shown to be sensitive to mutagenesis and important for receptor binding (Hébert *et al.*, 1991). The side chain of Ile-28, which occupies excellent electron density in our structure, has only one contact within 4.0 Å (Lys-29 C-δ) and is sufficiently exposed to interact directly with the receptor.

Activation of NAP-2—β-TG, CTAP-III, and PBP, which differ from NAP-2 only in having an additional 11, 15, and 24 residues, respectively, added to the amino terminus, are all inactive toward the IL-8 receptors at physiological concentrations (Walz *et al.*, 1989). The longer isoforms, which predominate in quiescent platelets, are converted to NAP-2 by cathepsin G, which cleaves the Tyr-21–Ala-22 peptide bond and releases the activation peptide. The system has strong positive feedback in that NAP-2 activates neutrophils, which release cathepsin G (Cohen *et al.*, 1992), which in turn activates platelets. Since a longer amino terminus does not induce a detectable change in the secondary structure of the NAP-2 portion (Yang *et al.*, 1994), it is likely that the extended amino-terminal chain inhibits by blocking access to one or more of the sites on NAP-2 that bind the receptor. The neural network method of Holley and Karplus (1989) predicts a turn of α-helix in the activation peptide consisting of Glu-12 to Asp-16. This predicted structure places two acidic groups on the same side of the helix, where they could interact with a positive residue such as Arg-24 (Fig. 6).

The activation peptide present in β-thromboglobulin (residues 10–20) has a provocative similarity to the amino-terminal extracellular domain of the IL-8 receptor in having a high concentration of acidic residues. Clubb *et al.* (1994) have proposed from NMR data that the receptor peptide, which has nine acidic residues among 40 positions for the type I receptor and 12 acidic residues among 49 for the type II receptor, binds to IL-8 in the cleft between residues 30–38 {residues 12–21} and the third strand of β-sheet, where it could interact with a cluster of basic residues. NAP-2 has three conserved residues whose basic side chains project into this region, namely Lys-29, Lys-37, and Arg-64.

Another similarity between the activation peptide in β-TG and the amino-terminal extracellular domain of the IL-8 type II receptor is the prediction that residues 43–46 (ESLE) of the receptor have the same helical structure, with two acidic groups on the same side of the helix, as predicted for the activation peptide. Moreover, residues 43–46 are in the one stretch of the receptor sequence that exhibits significant simi-
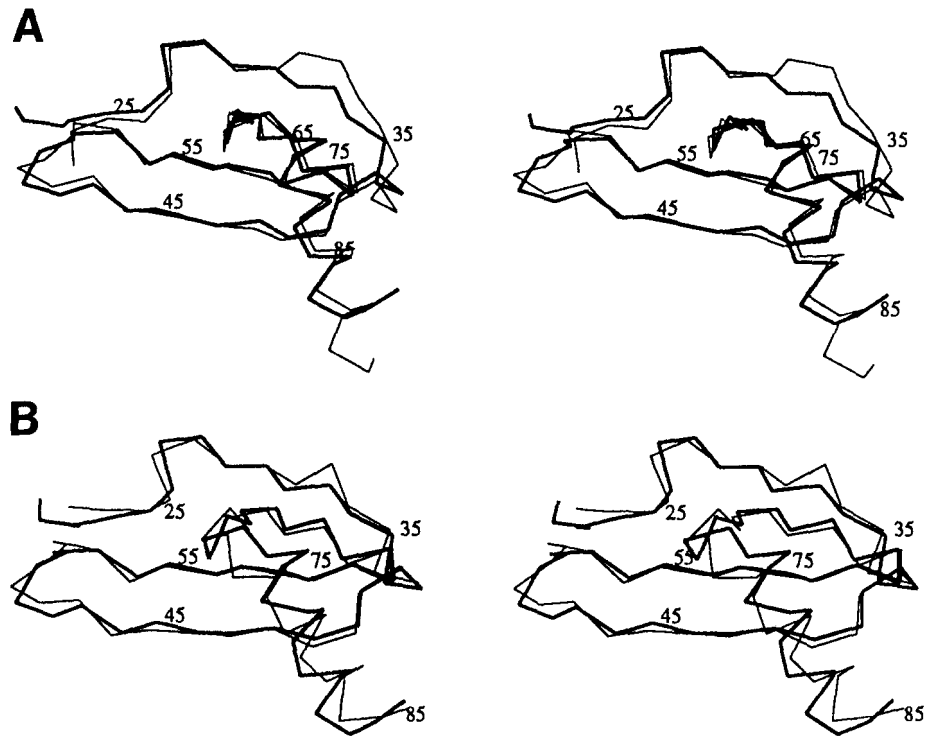
A

B

FIG. 7. **Comparison of NAP-2 with IL-8 and PF4.** The α-carbon backbone of subunit B of NAP-2 (*thick lines*) is compared with that of IL-8 (*A, thin lines*; x-ray structure) and human PF4 (*B, thin lines*). The superpositions were calculated with residues 23–86 and 24–85, respectively.

larity to the sequence of the activation peptide. The predicted α-helical region in the receptor peptide lies near the first transmembrane α-helix in the proposed receptor structure (LaRosa *et al.*, 1992). Therefore, cleavage of β-TG or a longer precursor into NAP-2 not only would remove the residues blocking the ELR sequence or other subsite, but would also allow the newly exposed amino terminus of NAP-2 to approach the receptor membrane closely and to interact with the putative α-helix in the receptor sequence. The type I receptor, for which NAP-2 has a much lower affinity, is less similar in sequence to the activation peptide and cannot have a helix with two acidic residues on the same side. These predictions raise the intriguing possibility that the activation peptide mimics, at least in part, the receptor interactions with NAP-2.

However, extensive alanine scanning of the IL-8 type I receptor sequence did not find any critical acidic residues among the 40 residues of the amino-terminal extracellular domain (Hébert *et al.*, 1993; Leong *et al.*, 1994). Replacement of Thr-18, Pro-21, or Tyr-27 reduced significantly the binding constant for IL-8 but not the mobilization of calcium, while replacement of Cys-30, which is near the predicted helical region in the type II receptor (as the conserved Cys-40), abolished both binding and transduction. An additional 19 residues in the second, third, and fourth extracellular domains were also shown to be involved in IL-8 binding.

Comparison with Other Chemokine Structures—Together, the crystal structures of NAP-2 and IL-8 identify some of the nuances of the interaction between the chemokines and their receptors. Two types of human neutrophil receptors for IL-8, whose sequences are 77% identical, have been separately cloned and expressed in mammalian cells (Moser *et al.*, 1991; Holmes *et al.*, 1991; Murphy and Tiffany, 1991; Cerretti *et al.*, 1993). IL-8 activates both type I and II receptors while NAP-2, which has 44% identity to IL-8, activates only the type II receptors at equivalent concentrations, although at high concentration, it can completely displace bound IL-8 from the surface of neutrophils (Petersen *et al.*, 1994). In contrast, PF4 and γIP-10 activate neither receptor (Clark-Lewis *et al.*, 1993, 1994). However, when residues 22–43, 47–52, and 66 in γIP-10

are replaced by the equivalent residues in IL-8 {residues 4–22, 30–35, and 49}, the hybrid γIP-10 is as potent as IL-8 in activating neutrophils (Clark-Lewis *et al.*, 1994), which suggests that positions 22–43, 47–52, and 66 in the CXC chemokine sequence define the binding site(s) for both types of receptor. Of course, it is still possible that other residues, which by chance are identical in IL-8 and γIP-10, are also critical parts of an extended binding site. However, outside of the three subsites defined above, γIP-10 has only nine residues that are identical to those in IL-8, and of these, only one is on the surface in the IL-8 structure and accessible to a receptor molecule.

Consequently, the explanation for IL-8 binding strongly to both receptors but NAP-2 only binding tightly to the type II receptor probably lies in the structural or chemical differences in these three subsites. An upper limit for structural differences attributable to error and thermal motion can be calculated from the differences among the independently determined structures of the four NAP-2 subunits. The maximum average C-α displacement relative to subunit B is 0.58 ± 0.28 Å for subsite I (residues 25–39 in subunit C), 1.09 ± 0.58 Å for subsite II (residues 47–52 in subunit C), and 0.42 Å for subsite III (residue 66 in subunit A). The amino-terminal ELR residues, which have large differences among some subunits as discussed above, were omitted from these calculations.

By these criteria, the structure of NAP-2, as measured by C-α positions relative to those of IL-8, exceeds the average displacement by more than two standard deviations at positions 28 and 32–37 (Figs. 7 and 8) in subsite I, but at no positions in subsite II or III. Although four of the seven residues at positions 32–37 are identical between IL-8 and NAP-2, the structural differences are not surprising given the insertion of Pro-33A in the sequence of IL-8. This site is the strongest candidate for a structural difference excluding NAP-2 from binding to the type I receptor.

Gly-48 and Pro-49 are critical for maximal binding of IL-8 to its receptors (Clark-Lewis *et al.*, 1994). If these two residues in IL-8 are switched or replaced by the equivalent residues in γIP-10 (Ser-48 and Gln-49), binding is decreased 170-fold

FIG. 8. **Deviations in C-α atom positions.** The deviations between C-α *(Ca)* positions are shown for NAP-2 overlapped with the IL-8 x-ray structure *(top)* and the human PF4 structure *(bottom)*.

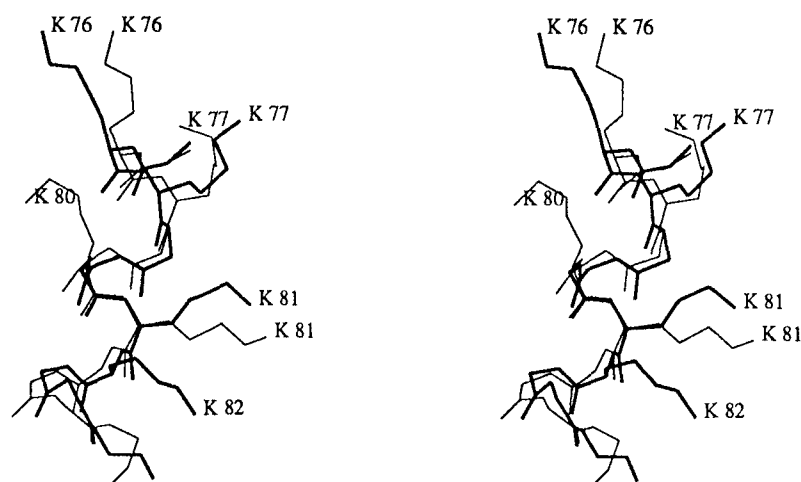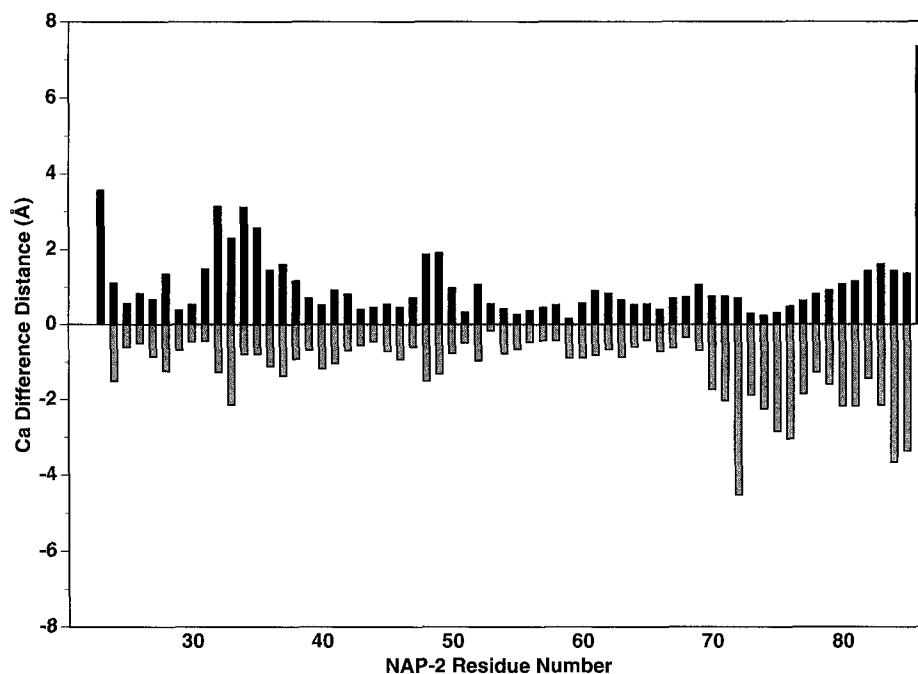
FIG. 9. **Comparison of the positively charged side chains in the carboxyl-terminal α-helix of NAP-2 and recombinant human PF4.** The main chain atoms for residues 75–85 and the side chain atoms for lysines 76, 77, 81, and 82 in the carboxyl-terminal α-helix of subunit B of NAP-2 *(thick lines)* are shown in stereo overlapped with the equivalent main chain atoms and the side chain atoms for residues 76, 77, 80, and 81 of recombinant human PF4 *(thin lines)*.

(Clark-Lewis *et al.*, 1994). Although residues 48 and 49 in NAP-2 are shifted by over 1.8 Å from those in IL-8, shifts of similar magnitude are seen among the NAP-2 subunits themselves. Because the chemokine structure is unusually flexible in this region, any effects of structural differences must be secondary to those caused by differences in sequence, namely the presence of Thr-49 in NAP-2 instead of the proline found in IL-8.

Surprisingly, mutagenesis of His-50 in IL-8 {H33} does not affect activity, in contrast to its immediate neighbors, Gly-48 {G31} and Pro-49 {P32} (Clark-Lewis *et al.*, 1994), although its side chain is near the ELR region in the IL-8 NMR structure, where it forms a hydrogen bond with Gln-26. A possible explanation lies in the NAP-2 structure, which shows that the His-50 side chain has two conformations available, one of which is buried. The side chains of His-50$_a$ (χ_1 = −54°) and His-50$_c$ (χ_1 = −48°) are solvent-accessible (side chain-accessible surface areas of 56.7 and 64.6 Å^2, respectively) and near the ELR region. His-50$_a$ forms two hydrogen bonds within the ELR segment (between the nitrogen of Arg-24$_a$ and the NE2 of His-50$_a$ and between the ND1 of His-50$_a$ and the oxygen of Glu-22$_a$). The only other residue in the NAP-2 tetramer, ex-

cluding contacts due to crystal packing, with side chain atoms within 4.0 Å of the ELR region is Thr-49$_a$, which contacts the side chain of Leu-23$_a$. The side chain of His-50$_c$ is in a similar conformation and within 3.5 Å of Arg-24$_c$, but the angles of the possible hydrogen bonds exceed the limits.

The side chain of His-50$_b$ (χ_1 = 63°) adopts a different conformation than that of His-50$_a$ and His-50$_c$ in that it points away from the ELR region and is buried within the core of the protein (solvent-accessible surface area of 3.9 Å^2). Specifically, the ND1 of His-50$_b$ forms an intersubunit hydrogen bond with the carbonyl oxygen of Gly-63$_d$. The His-50 side chains in the IL-8 x-ray structure and in three subunits of the PF4 tetramer have an orientation similar to that of His-50$_b$ in the NAP-2 structure. The side chain conformation of His-50$_d$ lies between that of His-50$_a$, His-50$_c$, and His-50$_b$, with a χ_1 angle of −47° and a solvent-accessible surface area of 41.9 Å^2. His-50$_d$ lies within 5.7 Å of the ELR region, but does not have contacts with it. However, the NE2 of His-50$_d$ does form an intersubunit hydrogen bond with the carbonyl oxygen of Asp-62$_b$.

The third region with significant structural differences among the CXC chemokines involves the α-helices at the carboxyl terminus of each subunit. In the crystal structures of

Structure of Neutrophil-activating Peptide-2 (M6L)

NAP-2 and IL-8 and the NMR structure of IL-8, the pair of antiparallel helices in the AB dimers (and CD dimers in NAP-2) traverse the extended β-sheets at an angle of approximately 58°. The distance between the helices in each pair is 8.5 Å for the crystal structures of NAP-2 and IL-8, but 10 and 11 Å for the crystal structure of bovine PF4 and the NMR structure of IL-8, respectively. Moreover, the helices of bovine and human PF4 are translated approximately 1.8 Å with respect to the helices in NAP-2 and IL-8 (Fig. 7B), which accounts for the larger than average root mean square deviation between the helical regions (Table II).

Mutagenesis studies have shown that residues 52–72 in IL-8, which include the carboxyl-terminal α-helix, are not directly involved in receptor binding or activation (Hébert *et al.*, 1991; Clark-Lewis *et al.*, 1991), but play a structural role instead. The helix has also been implicated in the binding of heparin to PF4 (Hardin and Cohen, 1976) and of heparin and heparan sulfate to IL-8 (Webb *et al.*, 1993). The binding of heparan sulfate to IL-8 increases the rate of chemotaxis by 3–4-fold and enhances Ca^{2+} release. Heparin had a similar effect on Ca^{2+} response, but did not enhance chemotaxis. The binding of IL-8 to heparan sulfate is abolished with the removal of residues 69–90 (Webb *et al.*, 1993). Although the heparin·IL-8 complex has a different overall charge and perhaps a slightly different conformation, the increased activity of IL-8 could also be due to the stabilization of IL-8 oligomers when the anionic polysaccharide binds across or between the pairs of helices.

Although no crystal structure exists of the complex between heparin and any chemokine, Stuckey *et al.* (1992) have proposed a model of heparin binding to bovine PF4 that predicts that seven basic residues, namely His-35, Lys-37, Lys-61, Lys-76, Lys-77, Lys-80, and Lys-81, interact with the negatively charged heparin chain that runs perpendicular to a pair of α-helices in a dimer. NAP-2 has Lys-80 replaced by glutamine and a new lysine at position 82, which dramatically changes the arrangement of positive charges in the helices (Fig. 9) as proposed by Lawler (1981). When NAP-2 is overlapped with bovine PF4 in the model of Stuckey *et al.* (1992), Lys-76 and Lys-82 do not interact with the heparin acidic groups, which would explain the weaker heparin binding of NAP-2 relative to PF4. Platelet basic protein, the precursor of NAP-2, elutes from a heparin-Sepharose column with 0.6–0.7 M NaCl (Holt and Niewiaroski, 1985), which is comparable to IL-8, which elutes from heparin columns at 0.5 M NaCl (Van Damme *et al.*, 1989).

REFERENCES

Baggiolini, M., and Clark-Lewis, I. (1992) *FEBS Lett.* **307**, 97–101

Baggiolini, M., Dewald, B., and Moser, B. (1994) *Adv. Immunol.* **55**, 97–179

Baker, E. N., and Hubbard, R. E. (1984) *Prog. Biophys. Mol. Biol.* **44**, 97–179

Baldwin, E. T., Weber, I. T., St. Charles, R., Xuan, J. C., Apella, E., Yamada, M., Matsusuma, K., Edwards, B. F. P., Clore, G. M., Gronenborn, A. M., and Wlodawer, A. (1991) *Proc. Natl. Acad. Sci. U. S. A.* **88**, 502–506

Bebawy, S. T., Gorka, J., Hyers, T. M., and Webster, R. O. (1986) *J. Leukocyte Biol.* **39**, 423–434

Begg, G. S., Pepper, D. S., Chesterman, C. N., and Morgan, F. J. (1978) *Biochemistry* **17**, 1739–1744

Bernstein, F. C., Koetzle, T. F., Williams, G. J. B., Meyer, E. F., Jr., Brice, M. D., Rodgers, J. R., Kennard, O., Shimanouchi, T., and Tasumi, M. (1977) *J. Mol. Biol.* **112**, 535–542

Bock, P. E., Luscombe, M., Marshall, S. E., Pepper, D. S., and Holbrook, J. J. (1980) *Biochem. J.* **191**, 769–776

Brandt, E., Petersen, F., and Flad, H.-D. (1993) *Mol. Immunol.* **30**, 979–991

Brunger, A. T. (1988) *J. Mol. Biol.* **203**, 803–816

Castor, C. W., Miller, J. W., and Walz, D. A. (1983) *Proc. Natl. Acad. Sci. U. S. A.* **80**, 765–769

Castor, C. W., Walz, D. A., Johnson, P. H., Hossler, P. A., Smith, E. M., Bignall, M. C., Aaron, B. P., Underhill, P., Lazar, J. M., Hudson, D. H., Cole, L. A., Perini, F., and Mountjoy, K. (1990) *J. Lab. Clin. Med.* **116**, 516–526

Cerretti, D. P., Kozlosky, C. J., van den Bos, T., Nelson, N., Gearing, D. P., and Beckman, M. P. (1993) *Mol. Immunol.* **30**, 359–367

Chambers, J. L., Ortega, R. B., and Campana, C. F. (1992) *50th Annual Meeting of the American Crystallographic Association*, August 9–14, 1992, Pittsburgh, PA, Vol. 20, p. 87, American Crystallographic Association, Buffalo, NY

Ciaglowski, R. E., Snow, J. W., and Walz, D. A. (1986) *Arch. Biochem. Biophys.* **250**, 249–256

Clark-Lewis, I., Schumacher, C., Baggiolini, M., and Moser, B. (1991) *J. Biol. Chem.* **266**, 23128–23134

Clark-Lewis, I., Dewald, B., Geiser, T., Moser, B., and Baggiolini, M. (1993) *Proc. Natl. Acad. Sci. U. S. A.* **90**, 3574–3577

Clark-Lewis, I., Dewald, B., Loetscher, M. T., Moser, B., and Baggiolini, M. (1994) *J. Biol. Chem.* **269**, 16075–16081

Clubb, R. T., Omichinski, J. G., Clore, G. M., and Gronenborn, A. M. (1994) *FEBS Lett.* **38**, 93–97

Clore, G. M., Appella, E., Yamada, M., Matsushima, K., and Gronenborn, A. M. (1990) *Biochemistry* **9**, 1689–1696

Cohen, A. B., Stevens, M. D., Miller, E. J., Atkinson, M. A. L, and Mullenbach, G. (1992) *Am. J. Physiol.* **63**, L249–L256

Deuel, T. F., Keim, P. S., Farmer, M., and Heinrikson, R. L. (1977) *Proc. Natl. Acad. Sci. U. S. A.* **4**, 2256–2258

Deuel, T. F., Senior, R. M., Chang, D., Griffin, G. L., Heinrikson, R. L., and Kaiser, E. T. (1981) *Proc. Natl. Acad. Sci. U. S. A.* **8**, 4584–4587

Dewald, B., Moser, B., Barella, L., Schumacher, C., Baggiolini, M., and Clark-Lewis, I. (1992) *Immunol. Lett.* **32**, 81–84

Furey, W., Wang, B. C., and Sax, M. (1982) *J. Appl. Crystallogr.* **15**, 160–166

Hardin, R. I., and Cohen, H. J. (1976) *J. Biol. Chem.* **251**, 4273–4282

Haskill, S., Peace, A., Morris, J., Sporin, S. A., Anisowicz, A., Lee, S. W., Smith, T., Martin, G., Ralph, P., and Sager, R. (1990) *Proc. Natl. Acad. Sci. U. S. A.* **87**, 7732–7736

Hébert, C. A., Vitangcol, R. V., and Baker, J. B. (1991) *J. Biol. Chem.* **266**, 18989–18994

Hébert, C. A., Chuntharapai, A., Smith, M., Colby, T., Kim, J., and Horuk, R. (1993) *J. Biol. Chem.* **268**, 18549–18553

Hermodson, M., Schmer, G., and Kurachi, K. (1977) *J. Biol. Chem.* **252**, 6276–6279

Holley, L. H., and Karplus, M. (1989) *Proc. Natl. Acad. Sci. U. S. A.* **86**, 152–156

Holmes, W. E., Lee, J., Kuang, W. J., Rice, G. C., and Wood, W. I. (1991) *Science* **253**, 1278–1280

Holt, J. C., and Niewiaroski, S. (1985) *Semin. Hematol.* **22**, 151–163

Hoogewerf, A., Leone, J., Reardon, I., Heinrikson, R., and Ledbettor, S. (1993) *Mol. Biol. Cell* **4**, (suppl.) 286 (abstr.)

Howard, A. J., Gilliland, G. L., Finzel, B. C., Poulos, T. L., Ohlendorf, D. H., and Salemme, F. R. (1987) *J. Appl. Crystallogr.* **20**, 383–387

Kabsch, W., and Sander, C. (1983) *Biopolymers* **22**, 2577–2637

Kungl, A. J., Machius, M., Huber, R., Schwer, C., Lam, C., Aschauer, H., Ehn, G., Lindley, I. J. D., and Auer, M. (1994) *FEBS Lett.* **347**, 300–303

LaRosa, G. J., Thomas, K. M., Kaufmann, M. E., Mark, R., White, M., Taylor, L., Gray, G., Witt, D., and Navarro, J. (1992) *J. Biol. Chem.* **267**, 25402–25406

Lawler, J. W. (1981) *Thromb. Res.* **21**, 121–127

Lenord, E. J., Yoshimura, T., Rot, A., Noer, K., Walz, A., Baggiolini, M., Walz, D. A., Goetzl, E. J., and Castor, C. W. (1991) *J. Leukocyte Biol.* **49**, 258–265

Leong, S. R., Kabakoff, R. C., and Hébert, C. A. (1994) *J. Biol. Chem.* **269**, 19343–19348

Luster, A. D., Unkeless, J. C., and Ravetch, J. V. (1985) *Nature* **315**, 672–676

Mayo, K. H., and Chen (1989) *Biochemistry* **28**, 9469–9478

Morris, A. L., MacArthur, M. W., Hutchinson, E. G., and Thornton, J. M. (1992) *Proteins Struct. Funct. Genet.* **12**, 345–364

Moser, B., Clark-Lewis, I., Zwahlen, R., and Baggiolini, M. (1990) *J. Exp. Med.* **171**, 1797–1802

Moser, B., Schumacher, C., von Tscharner, V., Clark-Lewis, I., and Baggiolini, M. (1991) *J. Biol. Chem.* **266**, 10666–10671

Moser, B., Dewald, B., Barella, L., Schumacher, C., Baggiolini, M., and Clark-Lewis, I. (1993) *J. Biol. Chem.* **268**, 7125–7128

Murphy, P. M., and Tiffany, H. L. (1991) *Science* **253**, 1280–1283

Oppenheim, J. J., Zachariae, C. O. C., Mukaida, N., and Matsushima, K. (1991) *Annu. Rev. Immunol.* **9**, 617–648

Park, K. S., Rifat, S., Eck, H., Adachi, K., Surrey, S., and Poncz, M. (1990) *Blood* **75**, 1290–1295

Petersen, F., Flad, H.-D., and Brandt, E. (1994) *J. Immunol.* **149**, 2467–2478

Peveri, P., Walz, A., Dewald, B., and Baggiolini, M. (1988) *J. Exp. Med.* **167**, 1547–1559

Poncz, M., Surrey, S., Larocco, P., Weiss, M. J., Rappaport, E. F., Conway, T. M., and Schwartz, E. (1987) *Blood* **69**, 219–223

Rajarathnam, K., Sykes, B. D., Kay, C. M., Geiser, T., Baggiolini, M., and Clark-Lewis, I. (1994) *Science* **264**, 90–92

Rao, S. N., Jih, J. H., and Hartsuck, J. A. (1980) *Acta Crystallogr. Sec. A* **36**, 878–884

Richardson, J. (1981) *Adv. Protein Chem.* **34**, 167–339

Rose, G., Gierasch, L. M., and Smith, J. A. (1985) *Adv. Protein Chem.* **37**, 1–109

Rossman, M. G., and Blow, D. M. (1962) *Acta Crystallogr.* **15**, 24–31

Satow, Y., Cohen, G. H., Padlan, E. A., and Davies, D. R. (1986) *J. Mol. Biol.* **190**, 593–604

Schnitzel, W., Monschein, U., and Besemer, J. (1994) *J. Leukocyte Biol.* **55**, 763–770

Sherry, B., and Cerami, A. (1991) *Curr. Opin. Immunol.* **3**, 56–60

Sibanda, B. L., and Thornton, J. M. (1985) *Nature* **316**, 170–174

St. Charles, R., Walz, D. A., and Edwards, B. F. P. (1989) *J. Biol. Chem.* **264**, 2092–2099

Stuckey, J. A. (1992) *Diss. Abstr.* **53**, 1034

Stuckey, J. A., St. Charles, R., and Edwards, B. F. P. (1992) *Proteins Struct. Funct. Genet.* **14**, 277–287

Tekamp-Olson, P., Gallegos, C., Bauer, D., McClain, J., Sherry, B., Fabre, M., Van Deventer, S., and Cerami, A. (1990) *J. Exp. Med.* **172**, 911–919

Van Damme, J., Van Beeumen, J., Conings, R., Decock, B., and Billiau, A. (1989) *Eur. J. Biochem.* **181**, 337–344

Waleh, N. S., Sohel, I., Lazar, J. B., Hudson, D. V., Sze, P., Underhill, P. A., and Johnson P. H. (1992) *Gene (Amst.)* **117**, 7–14

Walz, A., and Baggiolini, M. (1989) *Biochem. Biophys. Res. Commun.* **159**, 969–975

Walz, A., and Baggiolini, M. (1990) *J. Exp. Med.* **171**, 449–454

Walz, A., Dewald, B., von Tscharner, V., and Baggiolini, M. (1989) *J. Exp. Med.* **170**, 1745–1750

Walz, A., Burgener, R., Car, B., Baggiolini, M., Kunkel, S. L., and Strieter, R. M. (1991) *J. Exp. Med.* **174**, 1355–1362

Webb, L. M. C., Ehrengrber, M. V., Clark-Lewis, I., Baggiolini, M., and Rot, A. (1993) *Proc. Natl. Acad. Sci. U. S. A.* **90**, 7158–7162

Wolpe, S. D., Davatelis, G., Sherry, B., Beutler, B., Hesse, D., Nguyen, H. T., Moldawer, L. L., Nathan, C. F., Lowry, S. F., and Cerami, A. (1988) *J. Exp. Med.* **167**, 570–581

Yang, Y., Mayo, K. H., Daly, T. J., Barry, J. K., and La Rosa, G. J. (1994) *J. Biol. Chem.* **269**, 20110–20118

Zhang, K. Y. J. (1993) *Acta Crystallogr. Sec. D* **49**, 213–222

Zhang, X., Chen, L., Bancroft, D. P., Lai, C. K., and Maione, T. E. (1994) *Biochemistry* **33**, 8361–8366